JVSTA Journal of Vacuum Science & Technology A

Hydrogen contamination in Ge-doped SiO 2 thin films prepared by helicon activated reactive evaporation

W. T. Li, D. A. P. Bulla, J. Love, B. Luther-Davies, C. Charles, and R. Boswell

Citation: Journal of Vacuum Science & Technology A **21**, 792 (2003); doi: 10.1116/1.1570842
View online: http://dx.doi.org/10.1116/1.1570842
View Table of Contents: http://scitation.aip.org/content/avs/journal/jvsta/21/3?ver=pdfcov
Published by the AVS: Science & Technology of Materials, Interfaces, and Processing

Hydrogen contamination in Ge-doped SiO_2 thin films prepared by helicon activated reactive evaporation

W. T. Li,[a] D. A. P. Bulla, J. Love, and B. Luther-Davies
Australian Photonics CRC, Research School of Physical Science and Engineering, The Australian National University, ACT 0200, Australia

C. Charles and R. Boswell
Plasma Research Laboratory, Research School of Physical Science and Engineering, The Australian National University, ACT 0200, Australia

(Received 13 September 2002; accepted 10 March 2003; published 25 April 2003)

Germanium-doped silicon oxide thin films were deposited at low temperature by using an improved helicon plasma assisted reactive evaporation technique. The origins of hydrogen contamination in the film were investigated, and were found to be H incorporation during deposition and postdeposition water absorption. The H incorporation during deposition was avoided by using an effective method to eliminate the residual hydrogen present in the deposition system. The microstructure, chemical bonds, chemical etch rate, and optical index of the films were studied as a function of the deposition conditions. Granular microstructures were observed in low-density films, and were found to be the cause of postdeposition water absorption. The granular microstructure was eliminated and the film was densified by increasing the helicon plasma power and substrate bias during deposition. A high-density film was shown to have no postdeposition water absorption and no OH detected by using a Fourier-transform infrared spectrometer. [DOI: 10.1116/1.1570842]

I. INTRODUCTION

Ge-doped silicon oxide ($Ge–SiO_x$) thin films have been found to have all-color light, especially short wavelength emitting properties, and thus are expected to have important applications in optoelectronic devices.[1,2] Most importantly, the $Ge–SiO_x$ films have been widely used as the core material for the production of planar optical waveguides[3,4] because of their high optical transmission in the visible and infrared range, and also for their photosensitivity to UV light which enables direct writing of gratings or planar waveguide devices.

The $Ge–SiO_x$ films have been produced by flame hydrolysis,[5,6] low pressure chemical vapor deposition (LPCVD),[7] and plasma enhanced chemical vapor deposition (PECVD).[8,9] In all of these methods, either hydride gases such as SiH_4 and GeH_4 or organometallics such as tetraethyl-orthosilicate were used as the sources of Si and Ge. These gases are expensive and not easy to handle safely in production or experiment. In addition, both hydrolysis and LPCVD require a very high substrate temperature, which makes the integration of active electronic and optical components on the same chip impossible. Low-temperature deposition can be achieved by PECVD. However, the films produced by PECVD contain a large amount of hydrogen bonded in the form of Si—OH and Si—H,[10,11] which causes strong absorption bands at the wavelengths of 1370 nm and 1450 nm, hence limiting the bandwidth of the films as a waveguide core layer.

A helicon activated reactive evaporation (HARE) technique is presently used in our lab to produce the $Ge–SiO_x$ films, where pure solid sources of Si and Ge are evaporated into oxygen plasma to form the film, so that H contamination is ''theoretically'' avoided. Low-temperature deposition of the dense $Ge–SiO_x$ films is achieved by employing the advantage of a very high plasma density of a helicon source[12,13] and the feasibility of supplying an independent rf bias to the substrate. This deposition method and an investigation of H contamination in the films are presented in this article.

II. EXPERIMENT

A. Deposition system

The HARE device combines an evaporation source (electron beam) and a low pressure high-density helicon plasma source in a configuration where the evaporant is transported through the plasma source to condense on a substrate. The initial experimental setup of the HARE system has been previously described.[14,15] It had a limitation of depositing doped silica since it consisted of a single crucible electron-beam (e-beam) evaporator. If a mixture of Ge and Si is evaporated from the same crucible to form the $Ge–SiO_x$ films, due to different evaporation rates for Ge and Si at the same temperature, it is impossible to control the Ge doping level, and thus the refractive index of the deposited films. The updated HARE system is equipped with a electron gun (e gun) fitted with a hearth containing three crucibles. E-beam powers directed to each crucible can be controlled separately, and thus Si and Ge can be evaporated from two separate crucibles. In addition, for increasing the density of the film, an independent rf source was added to the system to bias the substrate. The substrate holder was water cooled, and the substrate temperature was below 200 °C during deposition.

[a]Electronic mail: weitang.li@anu.edu.au

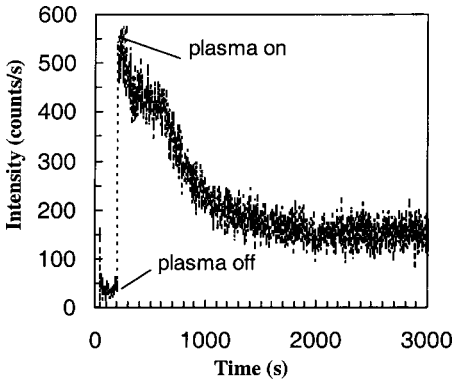

FIG. 1. Time-dependent variation of the hydrogen optical emission intensity during an Ar-plasma baking process.

B. Thin-film deposition

An Ar-plasma baking process was usually performed prior to the deposition to clean the Si substrate by ion bombardment, and to help water desorption from the inside walls of the reactor. The gas pressure was 4 mTorr and helicon rf power was 500 W during the Ar-plasma baking process. An optical emission spectrometer, named Monolite 6602, was used to monitor the H contamination in the processing chamber. Figure 1 shows a typical temporal evolution of the hydrogen optical emission intensity (HOEI) during the Ar-plasma baking process. The HOEI rapidly increases when the Ar plasma is turned on and gradually decreases toward a constant level after 1200 s. The stabilized HOEI level (150 counts/s) is owed to both the background of the optical emission of the plasma and remaining water vapor in the vacuum system.

After 20 min of Ar-plasma baking, small pieces of commercially available pure Si and Ge were first melted and then evaporated. The melting process was done within an oxygen and argon plasma, where the O_2 and Ar gas flows were set to 35 and 3 sccm, respectively, and the Ar was used only for stabilizing the plasma. Although the melting of the Si and Ge can be achieved in about 5 min, a special two-step extended melting process was used to eliminate H impurity in the raw Si and Ge materials. Figure 2 shows the temporal evolution of e-gun power and HOEI during the two-step melting process with the e-beam powers directed to the Si and Ge crucible fixed at a ratio of 2:1. As shown in Fig. 2, the HOEI increases with the rise of the e-beam power, and becomes stable when e-beam power is constant in the first melting step (100–700 s), then increases again at the beginning of second melting step, but subsequently decreases to its initial level ($t=0$) as a result of the removal of H impurity from the raw materials. A total melting time of ~1200 s is required by using this two-step process according to Fig. 2.

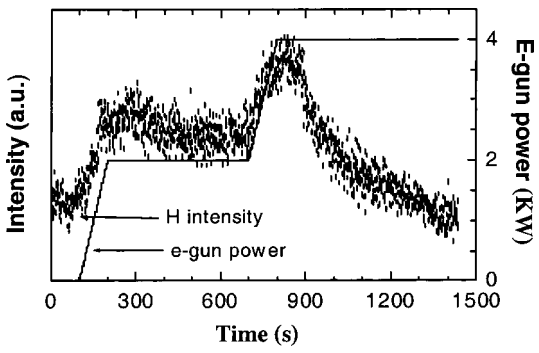

FIG. 2. Time-dependent variation of the hydrogen optical emission intensity and total e-gun power during the Ge and Si melting process.

Following the melting process, the deposition of Ge–SiO_x was started by further increasing the e-gun power to around 5 kW and removing the shutter covering the Si substrate during the melting process. In this study, the e-beam powers directed to Si and Ge during the deposition were chosen to be around 4.05 kW and 0.95 kW, respectively, which generated a Ge-doping level of ~1.4 wt% (according to a measurement of Rutherford backscattering spectrometry). The evaporation rates of Si and Ge usually decrease as the materials are consumed. To maintain constant evaporation rates for the two materials, it is necessary to monitor the evaporation rates and adjust the e-beam powers during deposition. The Si and Ge evaporation rates are monitored by using crystal rate sensors, and also by measuring the optical intensities of the Si and Ge atomic emission lines at wavelengths of 288 nm and 302 nm, respectively.

C. Thin-film characterization

The thin-film cross section and surface were viewed under a Hitachi 4500 field-emission scanning electron microscope (FESEM). The surface roughness of the samples was measured with a tapping mode atomic force microscope (AFM). The infrared transmission spectra of the films were recorded in the range of 400–4000 cm^{-1} using a Nicolet impact 400 Fourier-transform infrared (FTIR) spectrometer. The chemical etch rates of the films were determined using a *P*-etch solution [HF (40%): HNO_3 (70%) : $H_2O=3:2:60$]. Finally, the refractive index of the films was determined by using a J.A. Woollam M-44 ellipsometer.

III. RESULTS AND DISCUSSION

A. Microstructure

The FESEM observation revealed that the films deposited at a helicon plasma power $P<400$ W and without rf bias exhibit granular microstructures, as shown in Fig. 3(A) of the cross section of a film deposited with $P=200$ W, and in Fig. 3(B) of the surface of a film produced with $P=300$ W. The granular microstructure causes a large amount of voids within the films, and leads to low-density films. The granular microstructure was however not seen in the films deposited with $P>400$ W.

The surface roughness of the films was also investigated by using an AFM. Figure 4(A) exhibits the surface roughness of the films deposited with $P=200$ W and without rf bias. As seen in Fig. 4(A), the surface of the film is very rough and shows a granular structure again. When increasing the helicon plasma power to 500 W and supplying a substrate bias of

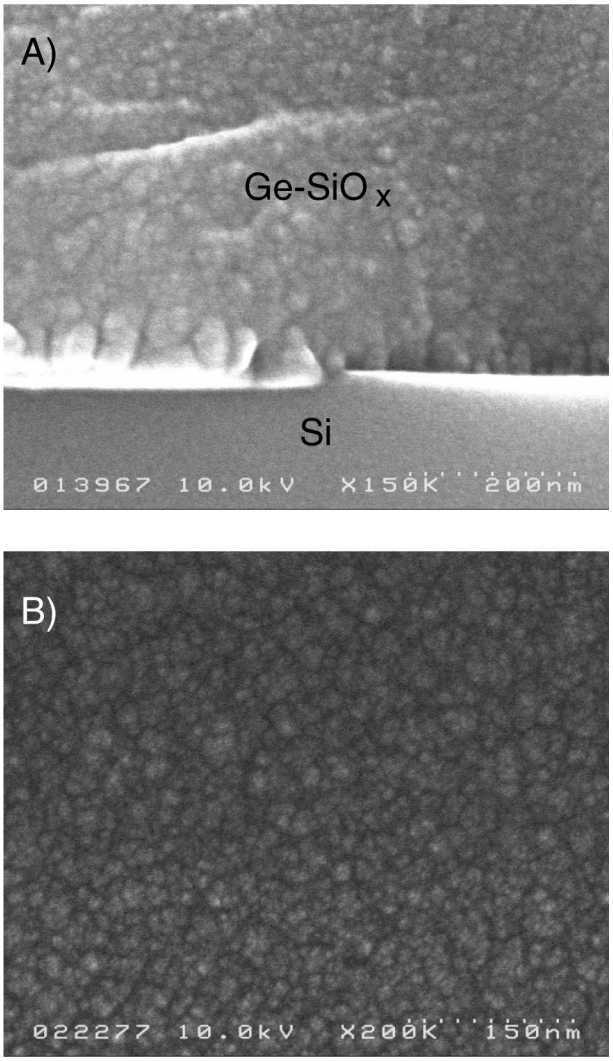

FIG. 3. FESEM images of (A) the cross-sections of a Ge–SiO_x film produced with a helicon rf power $P=200$ W, and (B) the surface of a Ge–SiO_x film prepared with $P=300$ W. No rf bias was applied to the two samples.

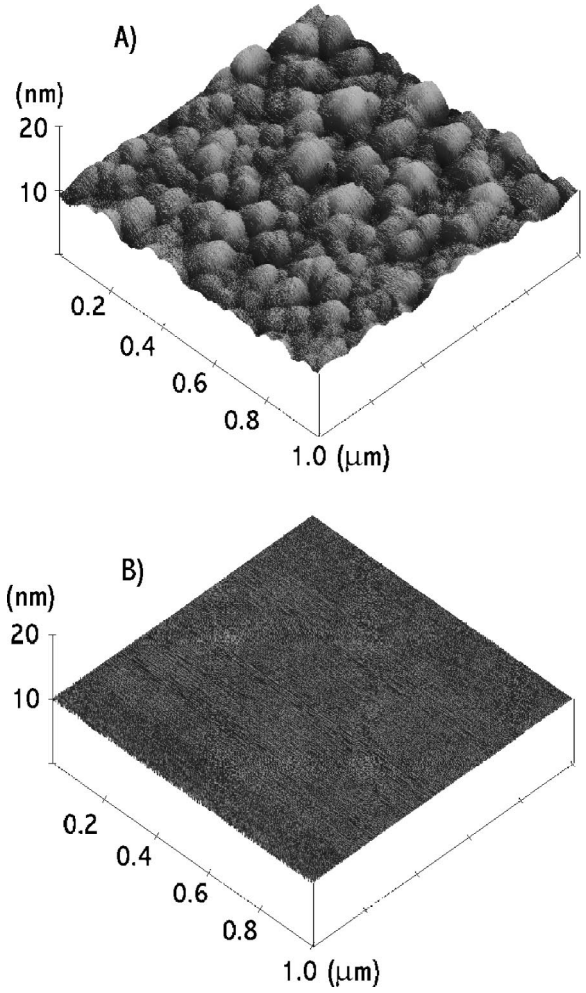

FIG. 4. Surface roughness obtained using an AFM for Ge–SiO_x films deposited under (A) helicon plasma power $P=200$ W, and no rf bias; (B) $P=500$ W, and substrate bias -170 V.

-170 V (dc offset of the rf bias), the surface of the deposited film became very smooth as shown in Fig. 4(B). Surface roughness is a known cause of surface scattering loss of a waveguide.[16] Low density, inhomogeneity, and defects of a waveguide material are the other major factors inducing the optical loss.[17] Choosing suitable helicon rf power and substrate bias to densify the film and improve the smoothness of the surface of the film is therefore very important for reducing the optical loss of the film.

B. Chemical bond

Figure 5 depicts the transmission FTIR spectra for two Ge–SiO_x thin-film samples (A and B). The two samples were prepared with the same helicon plasma power P (500 W) and substrate bias V_b (170 V). The gas flows and e-gun powers applied during the deposition for the two samples were also the same as specified in Sec. II. The only difference was that sample A was produced without the predeposition H elimination processes, which included the Ar-plasma baking pro-

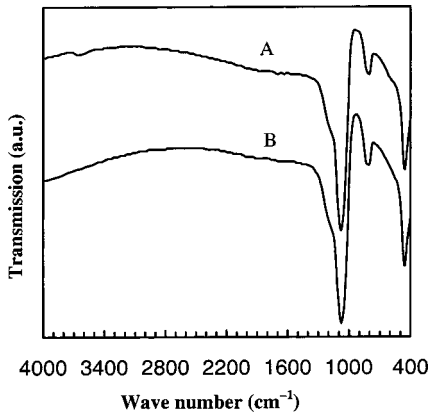

FIG. 5. FTIR transmission spectra of Ge–SiO_x films deposited with the same helicon plasma power (500 W) and substrate bias (-170 V). There were no predeposition H elimination processes applied to sample A, but there were to sample B.

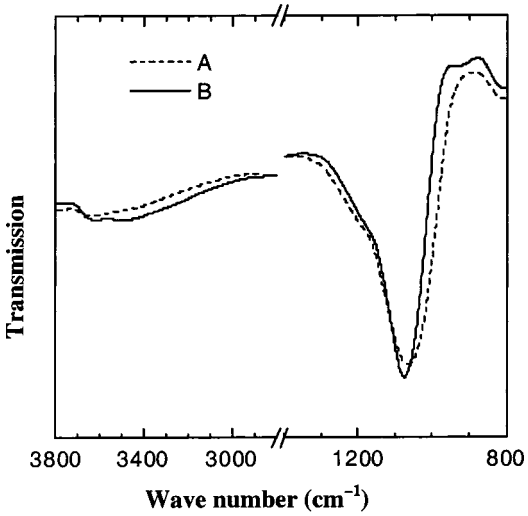

FIG. 6. FTIR spectra showing the effect of postdeposition water absorption for a low-density film produced with $P=200$ W. Spectrum A was taken within one day of depositing the film, and B was acquired after 2 months of exposure to room ambient (temperature ~25 °C, humidity 70%).

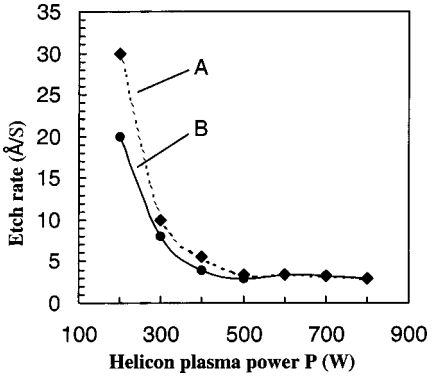

FIG. 7. *P*-etch rate of Ge–SiO_x films vs helicon rf power *P* in the case of no rf bias. Curve A was taken within one day of depositing the film, and B was acquired after 2 months of exposure to room ambient.

cess and the two-step melting process of the raw Si and Ge materials. As seen in Fig. 5, sample A exhibits Si—OH absorption bands at around 3650 cm^{-1}, but sample B does not. The two spectra were taken within one day of depositing the films, and showed no change after two months of exposure to air, revealing the absence of any postdeposition water absorption. Therefore, it can be concluded that the SiOH group in sample A was generated during the deposition since the predeposition H elimination processes were not performed. Ge—O absorption bands (near 870 and 580 cm^{-1})[18] are not clearly observed in the spectra due to the very low concentration of Ge (~1.4 wt %) in the films, and to the presence of rocking and bending of Si—O vibration modes at 450 cm^{-1} and 800 cm^{-1}.

H incorporation from postdeposition water absorption was observed in the Ge–SiO_x films presenting a granular microstructure. The films deposited with $P<400$ W have been shown to possess granular microstructures (Fig. 3), which provide a large fraction of voids and a greater surface to hold and react with water. In addition, GeO or GeO_2 itself is soluble in water and is likely to absorb water vapor from the air if the density of the Ge–SiO_x films is too low. Figure 6 exhibits the effect of postdeposition water absorption for a low-density film produced with $P=200$ W. Spectrum A was taken within one day of depositing the film, and spectrum B was acquired after 2 months of exposure to room ambient (temperature ~25 °C, humidity 70%). The hydrogen bonded SiOH groups around 3650 cm^{-1} in the two spectra are mainly generated during deposition since the predeposition H elimination processes were not used for this sample. In comparison with spectrum A, the water absorption bands around ~3330 cm^{-1} were enlarged and a SiOH band at ~935 cm^{-1} appears in spectrum B, showing that the film absorbed and reacted with water during the 2 months of exposure to humidity. In addition, the Si—O stretching band (near 1050 cm^{-1}) in spectrum B becomes narrower, and shifts to higher wave number in comparison with spectrum A. These effects are commonly observed phenomena for SiO_2 films when postdeposition water absorption occurs.[19] The broadness of the Si—O band is initially related to a high degree of strain and porosity of the films. Upon absorbing and reacting with water, the film becomes denser, the strain is relieved, and the variability in the bond force constants decreases, causing the Si—O stretching band to become narrower and shift to higher frequencies.[20,21]

For high-density films produced with $P>500$ W and substrate bias higher than 100 V, there is no FTIR measured evidence of postdeposition water absorption. Generally, the FTIR results show that it is possible for the HARE system to produce long-time stable Ge–SiO_x films with OH content less than the detection limit (0.1 wt %) of FTIR. This is an improvement compared to the PECVD Ge–SiO_x films that contain at least 0.55 wt % OH, and are deposited at a higher substrate temperature (300–400 °C).[10,22]

C. Chemical etch rate

P-etch solution, known to be sensitive to the density of silicon oxide films,[21] was used to measure the chemical etch rate of the Ge–SiO_x films. Figure 7 shows the etch rate versus the helicon plasma power applied for producing the films when no rf bias was used. Curve A, in Fig. 7, depicts the results obtained within one day of the deposition, and curve B represents the results acquired after 2 months of exposure to room ambient (temperature ~25 °C, humidity 70%). As seen from curve A, in Fig. 7, the etch rate decreases rapidly from 30 Å/s to 3 Å/s as *P* rises from 200 W to 500 W, indicating that the density of the film increases dramatically with the increase of *P* in this range. However, the etch rate does not reduce when further increasing *P* from 500 W to 800 W. A further reduction of the etch rate was obtained when increasing the substrate bias. A very low etch rate of ~2.4 Å/s, near that of thermal oxide (2 Å/s), was measured when supplying a substrate bias of over 150 V. This indicates that, besides increasing the helicon plasma power, an adequate substrate bias must be supplied for densifying the Ge–SiO_x films. Figure 7 also exhibits that there is an etch

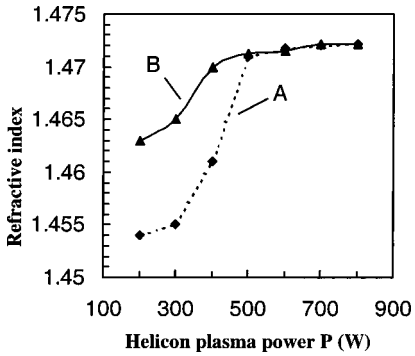

FIG. 8. Refractive index (at 632 nm) of Ge–SiO_x films vs helicon rf power P in the case of no rf bias. Curve A was taken within one day of depositing the film, and B was acquired after 2 months of exposure to room ambient.

rate reduction after 2 months of exposure to ambient for all the low-density films deposited with $P<500$ W. This can be explained by postdeposition water absorption-induced densification of the films and strain relief in the films.[21]

D. Refractive index

Figure 8 shows the refractive index (at 630 nm) of the films versus helicon plasma power applied for producing the films while keeping all the other deposition conditions the same. Curve A, in Fig. 8, was taken within one day of the film deposition, and curve B was acquired after 2 months of exposure to room ambient. The refractive index of a film usually increases with the increase of the density of the film and it is known to be a good measurement of the latter.[23] As seen from curve A, in Fig. 8, the index rapidly increases from 1.454 to above 1.47 when increasing P from 200 W to above 500 W, implying a large increase of the density of the film, which is in good agreement with the P-etch rate results (Fig. 7). Figure 8 also demonstrates that there is an index jump after two months of exposure to humidity for the low-density films deposited with $P<500$ W. This is more evidence of postdeposition water absorption. Upon absorbing and reacting with water, voids in a low-density film are filled, the density of the film increases, and thus its refractive index rises.

IV. SUMMARY

Nearly OH-free Ge–SiO_x films with a smooth surface and high density were deposited using an improved HARE technique. The H contamination in the films was found to occur both during and after deposition. Predeposition Ar-plasma baking of the reactor is found to be useful for water desorption from the walls of the vacuum system. A two-step long-time melting process of the raw evaporant materials can effectively remove the H impurity in the materials prior to evaporation. Performing these two predeposition H elimination processes minimizes H contamination in the films during deposition. Postdeposition water absorption was found in the low-density films presenting a granular microstructure. The investigation of the film microstructure, chemical bonds, chemical etch rates, and optical index revealed that increasing the helicon plasma power and substrate bias could effectively reduce the surface roughness of the film, increase the density of the film, and thus avoid postdeposition water absorption.

ACKNOWLEDGMENT

The authors are grateful to Dr. Cheng Huang for giving assistance with the FESEM application.

[1]X. L. Wu, T. Gao, G. G. Siu, S. Tong, and X. M. Bao, Appl. Phys. Lett. **74**, 2420 (1999).
[2]J. K. Shen, X. L. Wu, X. M. Bao, R. K. Yuan, J. P. Zou, and C. Tan, Phys. Lett. A **173**, 208 (2000).
[3]F. Bilodeau, B. Malo, J. Albert, D. C. Johnson, and K. O. Hill, Appl. Phys. Lett. **18**, 953 (1993).
[4]S. G. Blanco, A. Glidle, J. H. Davies, J. S. Aitchison, and J. M. Cooper, Appl. Phys. Lett. **79**, 2889 (2001).
[5]J. M. Ruano, V. Benoit, J. S. Aitchison, and J. M. Cooper, Anal. Chem. **72**, 193 (2000).
[6]G. D. Maxwell, R. Kashyap, B. J. Ainslie, D. L. Williams, and J. R. Armitage, Electron. Lett. **28**, 2106 (1992).
[7]S. Rastani and A. Reisman, J. Electrochem. Soc. **137**, 1288 (1990).
[8]J. S. Zhang, Z. X. Ren, R. Q. Liang, Y. F. Sui, and W. Liu, Surf. Coat. Technol. **131**, 116 (2000).
[9]M. V. Bazylenko, M. Gross, P. L. Chu, and D. Moss, Electron. Lett. **32**, 1198 (1996).
[10]M. V. Bazylenko, M. Gross, and D. Moss, J. Appl. Phys. **81**, 7497 (1997).
[11]K. Imoto and A. Hori, Electron. Lett. **29**, 1123 (1993).
[12]R. W. Boswell and R. K. Porteous, Appl. Phys. Lett. **50**, 1130 (1987).
[13]M. Koike and I. H. Suzuki, Jpn. J. Appl. Phys., Part 1 **34**, 6754 (1995).
[14]A. Durandet and R. W. Boswell, Rev. Sci. Instrum. **66**, 2908 (1995).
[15]B. Higgins, A. Durandet, and R. Boswell, J. Vac. Sci. Technol. B **13**, 192 (1995).
[16]R. M. Almeida, P. J. Morais, and H. C. Vaconcelos, Proc. SPIE **3136**, 296 (1997).
[17]R. G. Hunsperger, *Integrated Optics: Theory and Technology* (Springer, Berlin, 1984), p. 71.
[18]J. Y. Zhang, X. M. Bao, and Y. H. Ye, Thin Solid Films **323**, 68 (1998).
[19]W. A. Pliskin and P. P. Castrucci, Electrochem. Technol. **6**, 85 (1968).
[20]W. A. Pliskin and H. S. Lehman, J. Electrochem. Soc. **112**, 1013 (1965).
[21]W. A. Pliskin, J. Vac. Sci. Technol. **14**, 1064 (1977).
[22]M. V. Bazylenko, M. Gross, P. L. Chu, and D. Moss, Electron. Lett. **32**, 1198 (1996).
[23]A. Goullet, C. Vallee, A. Granier, and G. Turban, J. Vac. Sci. Technol. A **18**, 2452 (2000).